Brazilian Journal of Physics
ISSN: 0103-9733
luizno.bjp@gmail.com
Sociedade Brasileira de Física
Brasil

Kim, SeongMin; Ha, Jaewook; Kim, Jin-Baek
Ideal p-n Diode Current Equation for Organic Heterojunction using a Buffer Layer: Derivation and Numerical Study
Brazilian Journal of Physics, vol. 46, núm. 2, abril, 2016, pp. 170-174
Sociedade Brasileira de Física
São Paulo, Brasil

Braz J Phys (2016) 46:170–174
DOI 10.1007/s13538-016-0400-0

SOCIEDADE BRASILEIRA DE FÍSICA

GENERAL AND APPLIED PHYSICS

Ideal p-n Diode Current Equation for Organic Heterojunction using a Buffer Layer: Derivation and Numerical Study

SeongMin Kim[1,3] · **Jaewook Ha**[2] · **Jin-Baek Kim**[2]

Received: 10 May 2015 / Published online: 1 February 2016

Abstract The equation of p-n diode current-voltage (J-V) of an organic heterojunction (HJ) including a hole and electron buffer layer is derived, and its characteristics are numerically simulated based on a polaron-pair model Giebink et al. (Forrest, Phys. Rev. B **82**; 1–12, 2010). In particular, the correlation between a fraction of the potential drop for an electron/hole buffer ($\delta_{e-b}/\delta_{h-b}$) and for a donor (D)/acceptor (A) (δ_D/δ_A) is numerically investigated for J-V curves. As a result, the lowest diode current (DC) is obtained for the condition of $\delta_{e-b}+\delta_A \cong 0$ or $\delta_D+\delta_{h-b} \cong 1$. It is suggested that it is important to characterize the lowest DC curve for the state of D/A blending with a condition of a fraction of the potential drop ($\delta_{e-b}/\delta_{h-b}$). Under these circumstances, the transport of holes (h^+) from a DC source at the reverse bias is effectively limited.

Keywords Organic heterojunction · Buffer layers · p-n diode equation

1 Introduction

Electronic devices using organic semiconductors have extended the application fields of light-emitting diodes/displays [1–4], solar cells [5–9], organic field effect transistors [10–13], organic CMOS image sensors (OCIS) [14–17], and other technologies. In general, all of these devices consist of a p-n junction structure with bilayered or blending type of the active layers. To improve the performance of organic devices, an electron-transporting layer (ETL) or hole-transporting layer (HTL) is designed to add it or both into the system [18–20]. Particularly, in order to characterize the image sensor device (CIS) performance, diode current (DC) has been regarded as an important control parameter. This is because the reduction of DC is closely correlated with that of noises (e.g., shot noise or pattern noise of the system) [21, 22]. However, to reduce DC, it is rare to introduce electron and hole buffer layers into the organic-heterojunction OCIS system and then analytically derive DC equations to control a fraction of the potential drops of these buffer layers. This paper presents an analytic and numerical study of the DC reverse J-V characteristics of organic HJ devices using buffer layers. It is suggested that this method results in the lowest simulated DC.

2 J-V Model of Diode Current Using Buffer Layers

Our J-V characteristics are based on a polaron-pair model of organic heterojunctions, where recombination and generation (if excitons are considered) are used to govern currents in the system [23]. The schematic in Fig. 1 shows an energy-level diagram with anode and cathode injection barriers φ_a and φ_c, respectively. The barrier height between the donor and hole buffer layers and between the acceptor and electron buffer layers is denoted by φ_{h-b} and φ_{e-b}, respectively. The built-in potential is given by the work function difference between the cathode and

✉ SeongMin Kim
smkim417@hotmail.com

[1] The part of modeling AND simulation of device physics, The Office of Computational Energy Science (private lab), Maetan 3-dong, Yeongtong-gu, Suwon-si, Gyeonggi-do 443-373, South Korea

[2] Department of Chemistry, Korea Advanced Institute of Science and Technology, Daejeon 305-701, South Korea

[3] CAE, Platform Technology Lab, Samsung Advanced Institute of Technology, Suwon-si, Gyeonggi-do 443-803, South Korea

anode. Note that interface dipoles can exist anywhere between layers. The starting equation of diode current (J-V characteristics) in the presence of exponential trap density based on the polaron-pair model is shown below [1].

$$J = qa_o \frac{k_{ppr}}{k_{ppd}+k_{ppr}} \left\{ k_{rec,n}\left(n_I p_{It} - \frac{k_{ppd}}{k_{ppd,eq}} n_{I,eq} p_{It,eq} \right) + k_{rec,p}\left(p_I n_{It} - \frac{k_{ppd}}{k_{ppd,eq}} p_{I,eq} n_{It,eq} \right) \right\}. \quad \text{(M)}$$

where $k_{rec,n/p}$ describes a recombination between a free carrier with a trapped carrier at the HJ interface. (The recombination sites are at trap states.) The carrier densities at the HJ interface (n_I,p_I) are modeled via

$$p_I = p_{h-b} e^{q\delta_D (V_a - V_{bi})/kT} \quad (1)$$

$$p_{h-b} = p_c e^{q\delta_{h-b}(V_a - \varnothing_{h-b})/kT} \quad (2)$$

$$p_c = N_{HOMO} e^{-q\varnothing_a/kT} f(F_a, \mathrm{T}) \quad (3)$$

$$n_I = n_{e-b} e^{q\delta_A (V_a - V_{bi})/kT} \quad (4)$$

$$n_{e-b} = n_c e^{q\delta_{e-b}(V_a - \varnothing_{e-b})/kT} \quad (5)$$

$$n_c = N_{LUMO} e^{-q\varnothing_C/kT} f(F_c, \mathrm{T}), \quad (6)$$

where δ_D/δ_A is the fraction of the potential drop of donor/acceptor layers. V_a is the applied bias, k is Boltzmann's constant, T is the temperature, and V_{bi} is the built-in potential. q is the elementary charge, p_{h-b} is the hole density at the hole buffer layer, p_c is the hole density at the contact, and φ_{h-b} is the barrier height between hole buffer and donor layer. N_{HOMO} is the density of state (DOS) at the donor highest occupied molecular orbital (HOMO), φ_a is the injection barrier between the anode and the hole buffer layer, F_a is the electric field at the anode contact, and n_{e-b} is the electron density at the electron buffer layer. n_c is the electron density at the contact, φ_{e-b} is the barrier height between electron buffer layer and acceptor layer, N_{LUMO} is the DOS at the acceptor lowest unoccupied molecular orbit (LUMO), φ_c is the injection barrier between the cathode and the electron buffer layer, and F_c is the electric field at the cathode contact. δ_{h-b} is the fraction of the potential drop of the hole buffer layer and δ_{e-b} is the fraction of the potential drop of the electron buffer layer. Note that the term $f(F_a, \mathrm{T})/f(F_c, \mathrm{T})$ is associated with Schottky barrier lowering but here it is assumed to be one except in the presence of high electric fields and/or low temperatures [1]. For Eqs. 2 and 5, the density of hole buffer (p_{h-b}) and electron buffer (n_{e-b}) play a role of connecting interface density and contact density where a fraction of the potential drop of hole buffer (δ_{h-b}) and electron buffer (δ_{e-b}) and voltage drop of barrier height (φ_{e-b} or φ_{h-b}) are introduced into the Eqs. 2 and 5.

The trapped electron and hole densities at the HJ interface (n_t and p_t) are modeled via

$$n_t = N_{t,A} e^{\left[E_{trap}^{(n)} - E_{\mathrm{LUMO}}(V_a)\right]/kT_{t,A}} \quad (7)$$

$$p_t = N_{t,D} e^{\left[E_{\mathrm{HOMO}}(V_a) - E_{trap}^{(p)}\right]/kT_{t,D}} \quad (8)$$

$$n_{t,eq} = N_{t,A} e^{\left[E_{\mathrm{trap}}^{(n)} - E_{\mathrm{LUMO}}(0)\right]/kT_{t,A}} \quad (9)$$

$$p_{t,eq} = N_{t,D} e^{\left[E_{\mathrm{HOMO}}(0) - E_{\mathrm{trap}}^{(p)}\right]/kT_{t,D}}, \quad (10)$$

where $N_{t,A/D}$ is the density of the trap states at the acceptor/donor. $E^{(n/p)}{}_{\mathrm{trap}}$ is the trap energy level at the acceptor (n type)/donor(p type). E_{LUMO} is the LUMO energy of the acceptor, and E_{HOMO} is the HOMO energy of the donor. $T_{t,A/D}$ is the characteristic temperature for electron and hole trap distribution in the acceptor and donor. For Eqs. 7 and 8, the trap density energy level, $E^{(n/p)}{}_{\mathrm{trap}}$ is regarded as materials' characteristics which is independent of the external applied bias (V_a). The subscript eq. denotes the thermal equilibrium value in the absence of bias ($V_a = 0$).

Substituting above equations into the first part of Eq. (M) $\left(n_I p_{It} - \frac{k_{\mathrm{ppd}}}{k_{\mathrm{ppd,eq}}} n_{I,eq} p_{It,eq}\right)$ and the second part of Eqs. (M) $\left(p_I n_{It} - \frac{k_{\mathrm{ppd}}}{k_{\mathrm{ppd,eq}}} p_{I,\mathrm{eq}} n_{\mathrm{It,eq}}\right)$ yields

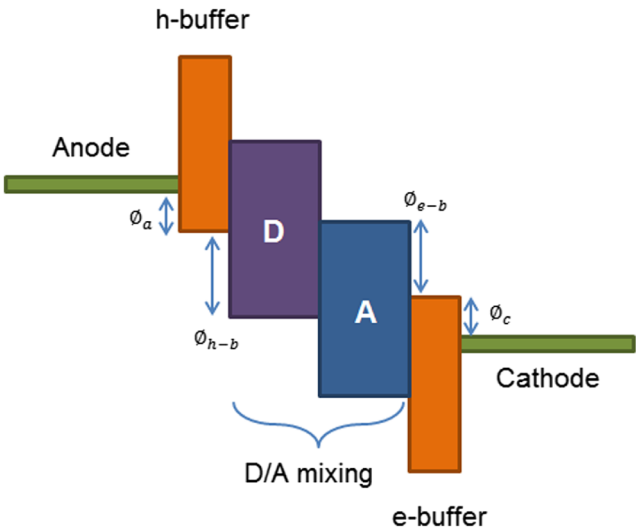

Fig. 1 A schematic of energy-level diagram of the anode, cathode, hole buffer layer (*h-buffer*), electron buffer layer (*e-buffer*), donor (*D*), and acceptor (*A*). Each barrier height is denoted by φ_a, φ_{h-b}, φ_{e-b}, φ_c etc

$$N_{\mathrm{LUMO}}^{\mathrm{cathode}} e^{q[-\varnothing_c-\delta_{e-b}\varnothing_{e-b}-\delta_A V_{bi}]/kT} N_{t,D} e^{\left[E_{\mathrm{HOMO}}(0)-E_{\mathrm{trap}}^{(P)}\right]/kT_{t,D}} \cdot \left\{ e^{qV_a/n_D kT} - \frac{k_{\mathrm{ppd}}}{k_{\mathrm{ppd,eq}}} \right\}, \tag{11}$$

where $q(\delta_{e-b}+\delta_A)V_a/kT+(E_{\mathrm{HOMO}}(V_a)-E_{\mathrm{HOMO}}(0))/kT_{t,D}=qV_a/n_DkT$

$$N_{HOMO}^{anode} e^{q[-\varnothing_a-\delta_{h-b}\varnothing_{h-b}-\delta_D V_{bi}]/kT} N_{t,A} e^{\left[E_{trap}^{(n)}-E_{LUMO}(0)\right]/kT_{t,A}} \cdot \left\{ e^{qV_a/n_A kT} - \frac{k_{ppd}}{k_{ppd,eq}} \right\}, \tag{12}$$

where $q(\delta_{h-b}+\delta_D)V_a/kT+(E_{\mathrm{LUMO}}(0)-E_{\mathrm{LUMO}}(V_a))/kT_{t,A}=qV_a/n_AkT$

Therefore, Eq. M can be rewritten as

$$\mathrm{J} = J_{SD}\left\{ e^{qV_a/n_D kT} - \frac{k_{\mathrm{ppd}}}{k_{\mathrm{ppd,eq}}} \right\} + J_{SA}\left\{ e^{qV_a/n_A kT} - \frac{k_{\mathrm{ppd}}}{k_{\mathrm{ppd,eq}}} \right\}, \tag{13}$$

with

$$\left\{ \begin{array}{l} J_{SD} = qa_0 \dfrac{k_{\mathrm{ppr}}}{k_{ppd}+k_{\mathrm{ppr}}} k_{\mathrm{rec},n} \left[N_{\mathrm{LUMO}}^{\mathrm{cathode}} e^{q[-\phi_c-\delta_{e-b}\phi_{e-b}-\delta_A V_{bi}]/kT} N_{t,D} e^{\left[E_{HOMO}(0)-E_{\mathrm{trap}}^{(p)}\right]/kT_{t,D}} \right] \\ J_{SA} = qa_0 \dfrac{k_{\mathrm{ppr}}}{k_{\mathrm{ppd}}+k_{\mathrm{ppr}}} k_{\mathrm{rec},p} \left[N_{\mathrm{HOMO}}^{\mathrm{anode}} e^{q[-\phi_a-\delta_{n-b}\phi_{n-b}-\delta_D V_{bi}]/kT} N_{t,A} e^{\left[E_{\mathrm{trap}}^{(n)}-E_{LUMO}(0)\right]/kT_{t,A}} \right] \end{array} \right\} \tag{14}$$

Note that n_D, n_A is an index of how closely the given diode can follow the ideal diode equation for donors (n_D) and acceptors (n_A), respectively.

If donors and acceptors are blended and each interface is denoted by i-th interface, the Eq. 13 can then be written as

$$J^{tot} = \sum_{i=1}^{n} J^i = \sum_{i=1}^{n} J_{SD}^i \left\{ e^{qV_a/n_D^i kT} - \frac{k_{ppd}}{k_{ppd,eq}} \right\} + \sum_{i=1}^{n} J_{SA}^i \left\{ e^{qV_a/n_A^i kT} - \frac{k_{ppd}}{k_{ppd,eq}} \right\} \tag{15}$$

$$= J_0^{tot} \left\{ e^{qV_a/n^{tot}kT} - \frac{k_{ppd}}{k_{ppd,eq}} \right\}, \tag{16}$$

From the above equations,

$$J_0^{tot} = \sum_{i=1}^{n} \left[J_{SD}^i + J_{SA}^i \right] \tag{17}$$

$$n^{tot} = \frac{qV_a}{kTln\left\{ 1 \dfrac{\sum_{i=1}^{n} J_{SD}^i e^{qV_a/n_D^i kT} + \sum_{i=1}^{n} J_{SA}^i e^{qV_a/n_A^i kT}}{J_0^{tot}} \right\}}. \tag{18}$$

For Eqs. 15 and 16, it is assumed that the blending forms a finite number of interfaces which then contribute as a sum to total current density for the blending consisting of n type and p type, because Eqs. 13 and 14 correspond to the current density J consisting of a n/p bilayer.

If the blending ratio is 1:1 (donors:acceptors), and n_A^i and n_D^i are equal for all the states assuming that the donor and the acceptor phases of the system have the same electrical conductivities (i.e., the same charge carrier mobilities), we can write the Eqs. 17 and 18 as

$$J_0^{tot} = \frac{J_0^{tot}}{2} + \frac{J_0^{tot}}{2} \tag{19}$$

$$n^{tot} = \frac{qV_a}{kTln\left\{\frac{1}{2}\left[e^{qV_a/n_AkT} + e^{qV_a/n_DkT}\right]\right\}}, \quad (20)$$

where

$$\frac{qV_a}{n_DkT} = \mathrm{q}(\delta_{e-b} + \delta_A)V_a \Big/ kT - qV_a \Big/ kT_{t,D} \quad (21)$$

$$\frac{qV_a}{n_AkT} = \mathrm{q}(\delta_{h-b} + \delta_D)V_a/kT + qV_a/kT_{t,A}. \quad (22)$$

The energy of the HOMO and LUMO is considered from the vacuum level. So $E_{\mathrm{HOMO}}(V_a) - E_{\mathrm{HOMO}}(0) = -qV_a$ and $E_{\mathrm{LUMO}}(0) - E_{\mathrm{LUMO}}(V_a) = qV_a$ are taken from Eqs. 21 and 22. The Eq. 19 is based on the average effects where each donor and acceptor share 1/2 of measured value such as $J_0^{\mathrm{tot}} = \frac{J_0^{\mathrm{tot}}}{2}(\mathrm{donors}) + \frac{J_0^{\mathrm{tot}}}{2}(\mathrm{acceptors})$

Substituting Eqs. 20–22 into Eq. 16 yields

$$\frac{J^{tot}}{J_0^{tot}} \cong \frac{1}{2}\left\{1e^{V_a\left[38.7\left(\delta_{h-b}+\delta_D\right)+11.6\right]} + e^{V_a\left[38.7\left(\delta_{e-b}+\delta_A\right)-11.6\right]}\right\} - 1, \quad (23)$$

with $T = 300$ K, $T_{t,A} = T_{t,D} = 1000$ K. By simplifying the effect of series and shut resistances, Eq. 23 can be rewritten as

$$\frac{J^{tot}}{J_o^{tot}} \cong \frac{1}{2}\left\{1e^{(V_a-J)\left[38.7\left(\delta_{h-b}+\delta_D\right)+11.6\right]} + e^{(V_a-J)\left[38.7\left(\delta_{e-b}+\delta_A\right)-11.6\right]}\right\} + (V_a - J) - 1. \quad (24)$$

Eq. (24) can be rewritten as

$$\mathrm{J} \cong \frac{1}{2}\left\{1e^{(V_a-J)\left[38.7\left(1-X\right)+11.6\right]} + e^{(V_a-J)[38.7X-11.6]}\right\} + V_a - J - 1, \quad (25)$$

with constraint of $\delta_{h-b} + \delta_D + \delta_{e-b} + \delta_A = 1$ where $\mathrm{X} \equiv \delta_{e-b} + \delta_A$

The Eq. (25) can be approximated as shown below in case of $\mathrm{X} \ll 0.5$ (ie. $\mathrm{X} \cong 0$)

$$\mathrm{J} \cong \frac{1}{2}\left\{e^{(V_a-J)50.3} + e^{-(V_a-J)11.6}\right\} + V_a - J - 1. \quad (26)$$

In case of $\mathrm{X} \gg 0.5$ (i.e., $\mathrm{X} \cong 1$), the Eq. (25) can be approximated as stated below

$$\mathrm{J} \cong \frac{1}{2}\left\{e^{(V_a-J)11.6} + e^{(V_a-J)27.1}\right\} + V_a - J - 1. \quad (27)$$

The reverse J-V model is based on the thermal generation currents from the depletion area

$$J_R \sim \frac{qn_i}{\tau_{gen}} W \cong k\sqrt{V_a}, \quad (28)$$

where n_i is the intrinsic concentration of the material, τ_{gen} is the generation life time, and W is the depletion width which is dependent on the square root of the applied voltage[22]. Note that k is a proportionality factor and equals 10^{-1}. It is assumed that once the materials are blended, a p/n junction is formed due to the phase separation where the difference of each donor and acceptor concentration determines the depletion width. This width is proportional to $\sqrt{V_a}$ on average. During simulation, the J-V curve used is continuous at $V_a = 0$, although the model used is different at different biases.

3 Simulation Results and Discussion

Figure 2 shows a calculated diode current density (J)-voltage(V) characteristics over the range from 0 to 1, using Eqs. 26 and 27 with the constraint of $\delta_{h-b} + \delta_D + \delta_{e-b} + \delta_A = 1$ where $\mathrm{X} \equiv \delta_{e-b} + \delta_A$. The plots show a correlation between $\delta_{e-b} + \delta_A$ (X) and $\delta_D + \delta_{h-b}$ (1-X); Based on these numerical results, the lowest DC is suggested to occur under the condition that $\delta_{e-b} + \delta_A \cong 0$ or $\delta_D + \delta_{h-b} \cong 1$. Conversely, for the highest DC following condition that $\delta_{e-b} + \delta_A \cong 1$ or $\delta_D + \delta_{h-b} \cong 0$ is occurred. Particularly, at the reverse bias the transport of the holes (h^+: from the source of DC generated at defects) through the hole buffer layer can be limited under the condition shown in Fig. 2 where $\mathrm{X} = 0$. Otherwise ($\mathrm{X} = 1$), increasing DC is shown. Based on the simulation results for the optimum condition for the lowest diode current (DC), it is suggested that under 1:1 blending (D:A) $\delta_{e-b} + \delta_A \cong 0$ or $\delta_D + \delta_{h-b} \cong 1$ is required. To fabricate a device requiring such a condition, an donor and a hole buffer layer

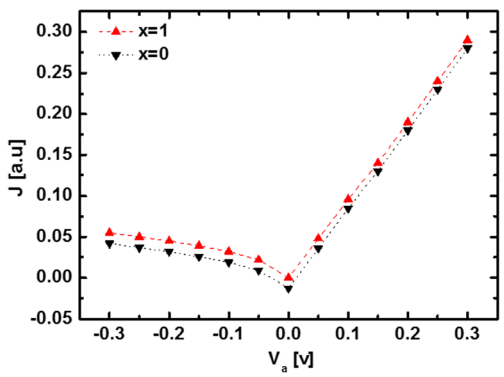

Fig. 2 A calculated diode current J-V plot with different fractions of potential drops of buffer layers and D/A layers under a condition of $\mathrm{X} = 0$ and $\mathrm{X} = 1$. Note that $\delta_A + \delta_D + \delta_{\eta-b} + \delta_{e-b} = 1$ where $X \equiv \delta_{e-b} + \delta_A$ showing the lowest diode current curve with $\mathrm{X} = 0$

should be highly doped materials (i.e., highly p doped donor and highly p-doped hole buffer layer). The reason for this is that the interaction between charged carriers and doped materials can lead to the electrostatic potential difference/drop effectively when passing through the doped materials at the reverse bias applied. This then leads to the lowest leakage current for the system. This paper represents two significant points: (1) numerical study of J-V characteristics on the organic HJ's diode currents using an electron and hole buffer layer in the system, and (2) particularly, study on the correlation between a fraction of the potential drop for an electron/hole buffer layer and D/A (donor/acceptor) layers, and suggestion on the DC reduction model/simulation. Diode current (DC) is associated with dark current (without photoexCitation) which is closely related with noise reduction in OCIS (organic CMOS image sensor) etc. This implies efficient image processing possible. This paper, thus, suggests a model/simulation to solve problems being addressed: how to reduce DC using buffer layers fundamentally in electronic imaging systems.

4 Conclusions

In this paper, the analytic equation of diode J-V characteristics of an organic heterojunction consisting of a buffer layer is derived and studied. As a result of numerical simulation, under reverse bias, the lowest DC is determined for the following condition: $\delta_{e-b}+\delta_A \cong 0$ or $\delta_D+\delta_{h-b} \cong 1$. This mathematical model can be used to understand and control/reduce DC for various optoelectronic devices.

Acknowledgments This work is supported by the office of computational energy science, Korea.

Compliance with Ethical Standards

Funding This study was not funded.

Conflict of interest The authors declare that they have no competing interests.

References

1. H. Uoyama, K. Goushi, K. Shizu, H. Nomura, C. Adachi, Nature **492**, 234–238 (2012)
2. M. Cai, T. Xiao, E. Hellerich, Y. Chen, R. Shinar, J. Shinar, Adv Mater **23**, 3590–3596 (2011)
3. Y. Tao, C. Yang, J. Qin, Chem Soc Rev **40**, 2943–2970 (2011)
4. G.M. Farinola, R. Ragni, Chem Soc Rev **40**, 3467–3482 (2011)
5. P.M. Beaujuge, J.M.J. Fréchet, J.M.J. Fr, J. Am, Chem Soc **133**, 20009–20029 (2011)
6. G. Li, R. Zhu, Y. Yang, Nat Photonics **6**, 153–161 (2012)
7. Y. Su, S. Lan, K. Wei, Mater Today **15**, 554–562 (2012)
8. C.J. Brabec, S. Gowrisanker, J.J.M. Halls, D. Laird, S. Jia, S.P. Williams, Adv Mater **22**, 3839–3856 (2010)
9. B.C. Thompson, P.P. Khlyabich, B. Burkhart, A.E. Aviles, A. Rudenko, G.V. Shultz, C.F. Ng, L.B. Mangubat, Green **1**, 29–54 (2011)
10. S. Kola, J. Sinha, H.E. Katz, J. Polym, Sci B Polym Phys **50**, 1090–1120 (2012)
11. C. Wang, H. Dong, W. Hu, Y. Liu, D. Zhu, Chem Rev **112**, 2208–2267 (2012)
12. J. Mei, Y. Diao, A.L. Appleton, L. Fang, Z. Bao, J. Am, Chem Soc **135**, 6724–6746 (2013)
13. J.D. Yuen, F. Wudl, Energy Environ Sci **6**, 392–406 (2013)
14. H. A. Mikio Ihama, Hideyuki Koguchi, Hiroshi Inomata, Y. H. Yuuki Imada, Yasuyoshi Mishima, Yoshihisa Kato, and S. K. Mizuki Segaw, Tetsuya Ueda, Proc. 16th Int. Disp. Work. Japan 2123 (2009).
15. T. M. Mikio Ihama, Hiroshi Inomata, Hideaki Asano, Shinji Imai, H. S. Yuuki Imada, Masayuki Hayashi, Takashi Gotou, and Y. M. Daigo Sawaki, Mitsumasa Hamano, Toshihiro Nakatani, Proc. 2011 Int. Image Sens. Work. Japan 153 (2011).
16. T. Watabe, S. Aihara, N. Egami, M. Kubota, K. Tanioka, N. Kamata, Proc. IEEE Work. Charg. Devices Adv. Image Sens. 48-51 (2005).
17. S. Takada, Proc SPIE **6068**, 60680A (2006)
18. T.H. Lai, S.W. Tsang, J.R. Manders, S. Chen, F. So, Mater Today **16**, 424–432 (2013)
19. Y. Shao, Y. Yang, Appl Phys Lett **83**, 2453–2455 (2003)
20. Y. Liao, X. Liu, J Electrochem Soc **157**, H759–H762 (2010)
21. N.V. Loukianova, H.O. Folkerts, J.P.V. Maas, D.W.E. Verbugt, A.J. Mierop, W. Hoekstra, E. Roks, A.J.P. Theuwissen, IEEE Trans Electron Devices **50**(77–83) (2003)
22. C. Zhang, S. Yao, J. Xu, J Semicond **32**, 115005 (2011)
23. N. Giebink, G. Wiederrecht, M. Wasielewski, S. Forrest, Phys Rev B **82**, 1–12 (2010)